Catalytic Reduction of Organohalide Pollutants by Myoglobin in a Biomembrane-like Surfactant Film

Alaa-Eldin F. Nassar, James M. Bobbitt, James D. Stuart, and James F. Rusling*

Contribution from the Department of Chemistry, Box U-60, University of Connecticut, Storrs, Connecticut 06269-3060

Received June 26, 1995[⊗]

Abstract: Stable, ordered films of myoglobin (Mb) and didodecyldimethylammonium bromide (DDAB) on electrodes were used to catalyze reductions of organohalides with significant lowering of activation free energy. Myoglobin in these films is made to act as a redox enzyme. Ethylene dibromide and trichloroacetic acid were dehalogenated by $MbFe^{II}$, with reaction rates much larger in the films than with $MbFe^{II}$ in solution. A highly reduced form of Mb was also produced in these films, and was used to dechlorinate tetra- and trichloroethylenes. All of these reactions occur at potentials about a volt more positive than the corresponding direct reductions at bare electrodes. Products were similar to those obtained from reduction by anaerobic bacteria or the enzyme cytochrome P450. Reactions proceeded for thousands of catalyst turnovers, and apparent rate constants were in the range 2×10^2 to 10^4 M^{-1} s^{-1}. Rates are partly enhanced by preconcentration of organohalides in the films. These ordered protein−surfactant films, featuring stacked surfactant bilayers, provide reaction environments resembling biomembranes.

Introduction

The heme protein myoglobin (Mb) is not primarily an electron carrier in living systems. However, Mb can catalyze organic oxidations[1−3] and reductions,[4−6] similar to the heme enzyme cytochrome P450.[7] Cytochrome P450 has been implicated in carcinogenic activation of pollutants,[7−12] and may be involved in microbial reductive dechlorinations in the environment.[13,14] Thus, the more readily available myoglobin provides a model for investigating the chemistry of pollutant activation and decomposition.

Dehalogenation of organic halides by reduced iron porphyrins and other heme-like transition metal complexes has been studied extensively. These reactions very often involve two-electron reduction to give simple hydrocarbons.[15−18] Examples include conversion of ethylene dibromide to ethylene[15a,d−g,16a,c] or chloroacetic acid to acetic acid.[16b]

We recently reported the direct electron transfer between electrodes and aquo-metMyoglobin [the Mb $heme Fe^{III}-H_2O$ form] in insoluble, ordered, liquid crystal surfactant films.[6,19−21] Electron transfer rates were up to 1000-fold larger between Mb and electrodes than for Mb in solution on bare Au, Pt, and carbon electrodes. A variety of water-insoluble surfactants were used to make stable Mb films with similar electron transfer properties. These films provide easy access to the Fe(II) form of Mb by injecting electrons from the electrode. Thus, reactions of the reduced protein with pollutant molecules can be studied easily using these films.

ESR anisotropy, polarized reflectance FT-IR, linear dichroism, and thermal phase transition studies showed that both Mb and surfactants are specifically oriented in the films. The surfactants

[⊗] Abstract published in *Advance ACS Abstracts*, October 15, 1995.

(1) Ortiz de Montellano, P. R.; Catalano, C. E. *J. Biol. Chem.* **1985**, *260*, 9265−9271.

(2) (a) Arduini, A.; Eddy, L.; Hochstein, P. *Arch. Biochem. Biophys.* **1990**, *281*, 41−43. (b) Rao, S. I.; Wilks, A.; Hamberg, M.; Ortiz de Montellano, P. R. *J. Biol. Chem.* **1994**, 269, 7210−7216.

(3) Kelman, D. J.; DeGray, J. A.; Mason, R. P. *J. Biol. Chem.* **1994**, *269*, 7458−7463.

(4) (a) Wade, R. S.; Castro, C. E. *J. Am. Chem. Soc.* **1973**, *95*, 231−234. (b) Bartnicki, E. W.; Belser, N. O.; Castro, C. E. *Biochemistry* **1978**, *17*, 5582−5586.

(5) Hamachi, I.; Noda, S.; Kunitake, T. *J. Am. Chem. Soc.* **1991**, *113*, 9625−9630.

(6) Rusling, J. F.; Nassar, A.-E. F. *J. Am. Chem. Soc.* **1993**, *115*, 11891−11897.

(7) (a) Ortiz de Montellano, P. R., Ed. *Cytochrome P450*; Plenum: New York, 1986. (b) Wislocki, P. G.; Miwa, G. T.; Lu, A. Y. H. In *Enzymatic Basis of Detoxication*; Jakoby, W. B., Ed.; Academic Press: New York, 1980; Vol. 1, pp 135−182.

(8) Guengerich, F. P.; MacDonald, T. L. *Acc. Chem. Res.* **1984**, *17*, 9−16.

(9) Dawson, J. H.; Sono, M. *Chem. Rev.* **1987**, *87*, *1255*−1276.

(10) Ingleman-Sundberg, M.; Johansson, I. *Biochemistry* **1980**, *19*, 4004−4011.

(11) Liebler, D. C.; Guengerich, P. F. *Biochemistry* **1983**, *22*, 5482−5489.

(12) DeVoss, J. J.; Ortiz de Montellano, P. R. *J. Am. Chem. Soc.* **1995**, *117*, 4185−4186.

(13) Castro, C. E.; Wade, R. S.; Belser, N. O. *Biochemistry* **1985**, *24*, 204−210.

(14) Li, S.; Wackett, L. P. *Biochemistry* **1993**, *32*, 9355−9361.

(15) (a) Wade, R. S.; Havlin, R.; Castro, C. E. *J. Am. Chem. Soc.* **1969**, *91*, 7530. (b) Wade, R. S.; Castro, C. E. *J. Am. Chem. Soc.* **1973**, *95*, 226−231. (c) Wade, R. S.; Castro, C. E. *J. Am. Chem. Soc.* **1973**, *95*, 231−234. (d) Lexa, D.; Saveant, J.-M.; Su, K. B.; Wang, D. L. *J. Am. Chem. Soc.* **1987**, *109*, 6464−6470. (e) Lexa, D.; Saveant, J.-M.; Su, K. B.; Wang, D. L. *J. Am. Chem. Soc.* **1988**, *110*, 7617−7625. (f) Lexa, D.; Saveant, J.-M.; Schafer, H. J.; Su, K.-B.; Vering, B.; Wang, D. L. *J. Am. Chem. Soc.* **1990**, *112*, 6162−6177. (g) Castro, C. E.; Yokohama, W. H.; Belser, N. O. *J. Agric. Food Chem.* **1988**, *36*, 915−919. (h) Helvenston, M. C.; Castro, C. E. *J. Am. Chem. Soc.* **1992**, *114*, 8490−8496.

(16) (a) Connors, T. F.; Arena, J. V.; Rusling, J. F. *J. Phys. Chem.* **1988**, *92*, 2810−2816. (b) Rusling, J. F.; Miaw, C. L.; Couture, E. C. *Inorg. Chem.* **1990**, *29*, 2025−2027. (c) Owlia, A.; Wang, Z.; Rusling, J. F. *J. Am. Chem. Soc.* **1989**, *111*, 5091−5098. (d) Zhou, D.-L.; Gao, J.; Rusling, J. F. *J. Am. Chem. Soc.* **1995**, *117*, 1127−1134.

(17) (a) Wackett, L. P.; Orme-Johnson, W. H.; Walsh, C. T. In *Metal Ions and Bacteria;* Beveridge, T. J., Doyle, R. J., Eds.; Acedemic Press: New York; 1989. (b) Gantzer, C. J.; Wackett, L. P. *Environ. Sci. Technol.* **1991**, *25*, 715−721. (c) Wackett, L. P.; Schanke, C. A. in *Metal Ions in Biological System*; Sigel, H., Sigel, A., Eds.; Marcel Dekker: New York, 1992. (d) Schanke, C. A.; Wackett. *Environ. Sci. Technol.* **1992**, *26*, 830−833. (e) Wackett, L. P.; Honek, J. F.; Begley, T. P.; Wallace, V.; Orme-Johnson, W. H.; Walsh, C. T. *Biochemistry* **1987**, 26, 6012−6018.

(18) Lovely, D. R.; Woodward, J. C.; Chapelle, F. H. *Nature* **1994**, *370*, 128−131.

(19) (a) Nassar, A-E. F.; Willis, W. S.; Rusling, J. F. *Anal. Chem.* **1995**, *67*, 2386−2392. (b) Rusling, J. F.; Nassar, A-E. F. *Langmuir* **1994**, *10*, 2800−2806.

(20) Nassar, A-E. F.; Narikiyo, Y.; Sagara, T.; Nakashima, N.; Rusling, J. F. *J. Chem. Soc., Faraday Trans.* **1995**, *91*, 1775−1782.

(21) Rusling, J. F.; Nassar, A-E. F.; Kumosinski, T. F. In *Molecular Modeling*; Kumosinski, T. F., Leibman, M. N., Eds.; ACS Symposium Series 576; American Chemical Society: Washington, DC, 1994; pp 250−269.

0002-7863/95/1517-10986$09.00/0

are arranged in stacked bilayers similar to lipid membranes.[6,20-22] Heme orientation was relatively independent of surfactant type or charge (i.e., +1, 0, −1), suggesting that Mb is at least partly imbedded in the surfactant bilayers. We felt that these films might provide good models to investigate chemical reactions of redox proteins in an environment resembling biomembranes.

Organohalides are widespread pollutants with varying degrees of toxicity.[23-25] In this paper, we report kinetics and product analyses for the reductions of several aliphatic halides catalyzed by Mb in films of cationic surfactant on an electrode. Both the Fe(II) form and a second, more highly reduced form of Mb are active reductants. Reaction rates were much larger in films than in solution, and may be enhanced by preconcentration of the organohalides into the surfactant film.

Experimental Section

Materials and Solutions. Horse skeletal muscle myoglobin from Sigma was dissolved in a pH 5.5 buffer (0.01 M acetate + acetic acid) containing 50 mM NaBr. Myoglobin solutions were passed through a YM30 filter (Amicon, 30 000 MW cutoff) to remove high MW impurities.[19a]

Ethylene dibromide (1,2-dibromoethane) (EDB), mono- and di- and trichloroacetic acid (TCA), and acetic-d_3 acid and its sodium salt were from Sigma. Tetrachloroethylene (PCE) [CCl_2=CCl_2] and didodecyldimethylammonium bromide (DDAB, 99%) were from Kodak, and trichloroethylene (TCE) [CHCl=CCl_2] was from Fisher. Hemin [chloroprotoporphyrin IX iron(III)] was from Aldrich. Water was purified with a Barnstead Nanopure system to specific resistance >15 MΩ·cm. All other chemicals were reagent grade.

Voltammetry. Methods and apparatus for cyclic voltammetry (CV) were described previously.[6,19,20] Basal plane, ordinary pyrolytic graphite (PG) disks (HPG-99, Union Carbide; geometric A = 0.2 cm^2) were abraded on 600-grit SiC paper prior to coating with films. Potentials are referred to the saturated calomel reference electrode (SCE).

For spectroelectrochemistry, films were cast onto transparent tin-doped In_2O_3 (ITO, CG-80IN-CUV, Delta Technol.). Absorption spectra were obtained with a Perkin-Elmer Lambda 6 UV−vis spectrophotometer.

Film Preparation. Method A:[6,19a] The required volume of 10 mM DDAB in chloroform, estimated from molecular volumes, to give film thicknesses of ca. 20 μm was spread evenly onto PG disks. Chloroform was evaporated overnight in air. Films were then equilibrated in buffers containing 0.5 mM Mb for several hours.

Method B:[19a] DDAB suspensions (10 mM) in water were ultrasonicated for four hours or more to produce clear vesicle dispersions.[26] Equal volumes of vesicle dispersion and 0.5 mM Mb in pH 5.5 buffer were mixed. An appropriate volume of this mixture was spread evenly onto electrodes to give film thicknesses of ca. 20 μm.

Bulk Electrolysis. Films using 50 μL of the Mb-DDAB vesicle dispersion (method B) were cast on both sides of a rectangular PG working electrode (1.0 cm × 1.0 cm × 0.3 cm). Approximately 15 nmol of Mb out of the 25 nmol deposited were found to be electroactive by Coulometric analysis[6] in pH 5.5 buffer.

Constant potential electrolyses were done in solutions stirred continuously in an undivided, gas tight cell containing a Pt coil counter electrode and an SCE reference. Solutions were purged with purified nitrogen for 20 min before and during electrolyses. The gas effluent from the cell was passed through a cold trap in liquid nitrogen. Deuterated acetate buffer was used to simplify NMR analyses.

The following concentrations were used: 25 mM TCA, 15 mM EDB, 12 mM [saturated] PCE, and 30 mM [saturated] TCE. Bulk electrolysis was done for 24 h with the working electrode potential (all vs SCE) at −0.4 V for TCA, −0.5 V for EDB, and −1.3 V for PCE and TCE. After electrolysis of TCA, PCE, and TCE, NaOH was added to pH 9.0, then procedures described below were used.

After electrolysis of TCA, water was distilled off. The residue was dissolved in D_2O and distilled again. The final residue was dissolved in 1 mL of D_2O and analyzed by NMR. For NMR analysis after electrolyses of PCE and TCE, a 3−4 mL deuterated chloroform extract was used. NMR was done by using a Bruker AC-270, 270-MHz spectrometer. Proton chemical shifts in ppm were as follows: acetate 1.86, monochloroacetate 4.05, dichloroacetate 5.93, TCE 6.5, and dichloroethylene 6.4.

Separate electrolyses of PCE and TCE were done for quantitative analysis by GC[27a] and GC-MS,[27b] using the static headspace method.[27a] Also, the effluent gas from the cell trapped at 77 K was analyzed.

During electrolysis of EDB, the entire effluent from the cell was collected in a 6 L evacuated vacuum canister (EPA method TO-14).[27c] This sample gave a single GC-MS product peak identified as ethylene (t_R 3.5 min).

GC-MS Analysis. A Tekmar ALS 2016 purge-and-trap apparatus and a Tekmar LSC 2000 concentrator were used with a Hewlett-Packard 5890 series II gas chromatograph with a cryogenic focusing capillary interface and an HP 5971 mass spectrometric detector. EPA method 8260 for analysis of volatile organic compounds[27b] was followed. GC conditions were the following: initial temperature 35 °C (1.0 min), final temperature 180 °C (16.87 min), temperature program rate 8.0 °C/min, injection temperature 180 °C, transfer line temperature 250 °C; column 1.8 μm DB-624 (J&W Scientific), length 60 m, and i.d. 0.32 mm.

A volume of 5.0 μL of a headspace or cold trapped sample was diluted in 5.0 mL of deionized water. This mixture was purged with helium, and the volatile organic compounds were analyzed. Internal standards and their retention times (t_R) were 1,2-dichloroethane (12.8 min), toluene (16.0 min), and 4-bromofluorobenzene (20.9 min). External reference standards were PCE (17.1 min), TCE (13.9 min), and (Z)-1,2-dichloroethene (11.5 min). Product analyses for TCE and PCE are reported as the sum of amounts found from the headspace and effluent gas. For the volatile EDB products, only the effluent gas was analyzed.

Alternative GC analyses were done by static headspace,[27a] to find saturation concentrations of TCE, PCE, and EDB in the buffer, and as a periodic check on GC-MS. A capillary GC-FID (Hewlett-Packard Model 5890) with a 30-m column, 0.55-mm i.d., 3.0 μm DB-1 (J&W Scientific), and a He flow rate 5−7 mL/min was used.

Rate Constant Estimations. CV was used to estimate formal potentials ($E^{o\prime}$), charge transport diffusion coefficients (D_{ct}), and apparent standard heterogeneous rate constants ($k^{o\prime}$) for Mb using methods described previously for these thick films.[6] Apparent chemical rate constants (k'_1) for reactions of reduced Mb with organohalides were estimated by CV with the aid of theoretical curves for two-electron electrocatalytic reductions[16d] computed by the digital simulation program[28] DigiSim 1.0 (BAS), as described previously.[16d]

Simulation models employed the measured parameters D, $E^{o\prime}$, and $k^{o\prime}$ for Mb-DDAB and an EC′ (electron transfer/catalytic chemical step) mechanism, using the solution electron transfer (SET) approximation to account for the second electron transfer.[16d,29] Theoretical curves were computed to relate catalytic efficiencies expressed as i_c/i_d to log (k_1'/v), where v = scan rate. The symbol i_c denotes the steady state peak catalytic CV current at coated electrodes in solutions of organohalides, and i_d is the peak CV current for Mb-DDAB in the absence of organohalide.

(22) Nassar, A-E. F.; Zhang, Z.; Chynwat, V.; Frank, H. A.; Rusling, J. F.; Suga, K. *J. Phys. Chem.* **1995**, *99*, 11013−11017.
(23) Travis, C. C.; Hester, S. T. *Environ. Sci. Technol.* **1991**, *25*, 815.
(24) Leisinger, T. *Experientia* **1983**, *39*, 1183−1191.
(25) Chaudry, G. R.; Chapalamadugu, S. *Microbiol. Rev.* **1991**, *55*, 59−79.
(26) Fendler, J. H. *Membrane Mimetic Chemistry*; Wiley: New York, 1982.
(27) (a) Robbins, G. A.; Wang, S.; Stuart, J. D. *Anal. Chem.* **1993**, *65*, 3113. (b) EPA Method 8260 in SW-846, *Test Methods for Evaluating Solid Waste;* U.S. Government Printing Office: Washington, DC, 1992; Physical Chemical Methods, Rev. 1. (c) EPA method TO-14, in SW-846, *Test Methods for Evaluating Solid Waste;* U.S. Government Printing Office: Washington, DC, 1992; Physical Chemical Methods, Rev. 1. (d) Rusling, J. F. *CRC Crit. Rev. Anal. Chem.* **1989**, *21*, 49−81.
(28) Rudolph, M.; Reddy, D. P.; Feldberg, S. W. *Anal. Chem.* **1994**, *66*, A589−A600.
(29) In the SET approximation, the second fast electron transfer following the rds is accounted for by doubling the experimental concentration of substrate in an EC′ simulation, see: Andrieux, C. P.; Blocman, C.; Dumas-Bouchiat, J.-M.; M'Halla, F.; Saveant, J.-M. *J. Electroanal. Chem.* **1980**, *113*, 19−40.

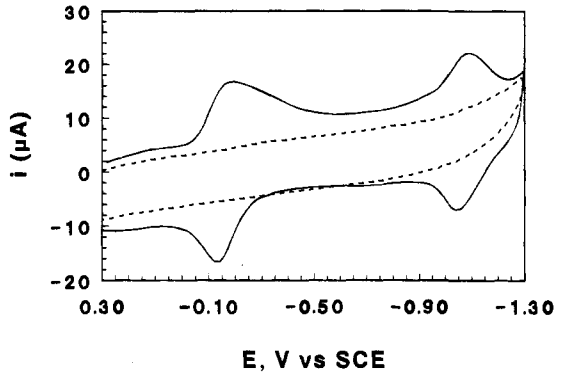

Figure 1. Steady state cyclic voltammograms at 100 mV s^{-1} in pH 5.5 buffer + 50 mM NaBr: dashed line, bare PG electrode with 0.5 mM Mb in solution; solid line, fully loaded Mb-DDAB film in buffer containing no Mb.

Simulations employed the diffusion coefficient of the substrate within the film at 10-fold greater than that of Mb, an assumption based on approximate molecular sizes. The measured concentration of electroactive Mb was used, with twice the organohalide concentration in solution according to the SET approximation.[29] This analysis provided apparent rate constants (k_1') which assume a unit partition coefficient into the films for all organohalides, since the actual organohalide concentration at the site of reaction is uncertain. Thus, k_1' values include a factor reflecting the actual partition coefficient of organohalide between films and solution.

Rate constants in solution were obtained under anaerobic conditions by measuring spectrophotometric changes in visible $MbFe^{II}$ Soret absorbance bands with time, as described by Castro et al.[4] $MbFe^{II}$ was produced by reduction of $MbFe^{III}$ with sodium dithionite. Pseudo-first-order conditions in $MbFe^{II}$ were maintained by using 10 μM myoglobin and 10 mM TCA or saturated (15 mM) EDB in pH 5.5 buffer. Rate constants were obtained by fitting absorbance vs time data to a first-order decay model using nonlinear regression.[27d]

Results

Myoglobin Voltammetry. CVs for Mb-DDAB films at 100 mV s^{-1} in pH 5.5 buffer containing no Mb (Figure 1) show two pairs of cathodic−anodic peaks. The peaks centered near −0.15 V vs SCE represent the $MbFe^{III}/Fe^{II}$ couple, as reported previously.[6,19,20] A second pair of peaks centered at about −1.1 V vs SCE suggests the reduction of $MbFe^{II}$ and reversible oxidation of the reduction product. One electron per electroactive Mb molecule is transferred in each peak.[27d]

Both sets of peaks display typical diffusion-kinetic controlled shapes (Figure 1) at scan rates above 50 mV s^{-1}. At these scan rates, the cathodic currents for both peaks were proportional to the square root of the scan rate (ν), as expected for diffusion-kinetic control[30] at the electrode−film interface.

Apparent standard heterogeneous rate constants for Mb-DDAB films were similar for first and second peaks, and much larger than values for Mb in solution on bare electrodes (Table 1). The formal potential from the second pair of peaks is −1.09 V vs SCE, similar to values of −1.03 to −1.06 V for Fe^{II}/Fe^{I} of tetraphenylporphyrin iron (TPPFe) in weakly complexing solvents containing Br^-.[31]

UV−Vis Spectroelectrochemistry. Absorption spectra of Mb-DDAB films on ITO electrodes showed distinct changes after each of a series of potentials were applied for 20 min. At 100 mV vs SCE, the $MbFe^{III}$ Soret band appears near 408 nm[32] (Figure 2). At −250 mV, close to the formal potential of $MbFe^{III}/Fe^{II}$ on ITO,[19] the $MbFe^{III}$ band decreased and a new peak at 432 nm was found. This peak is characteristic of $MbFe^{II}$,[33] and is the main peak at −500 mV, showing that nearly all of the Mb in the film was converted to $MbFe^{II}$. At −1250 mV, the 432-nm peak is replaced by a new peak at 411 nm. The $MbFe^{II}$ spectrum was again observed after 20 min at −500 mV.

The evolution of Mb-DDAB spectra with changing electrode potential resembles that reported for iron tetraphenylporphyrin derivatives.[31] Wavelength maxima for the Fe(III), Fe(II), and Fe(I) forms of these complexes (Table 2) change in a similar way to those of the Mb-DDAB films as potential becomes more negative. This comparison suggests, but does not prove, that the species formed at −1250 mV, beyond the second CV peak, may be an Fe(I) form of myoglobin.

Voltammetry of Organohalide Reductions. An increase in reduction peak current for $MbFe^{III}$ in Mb-DDAB films, accompanied by the disappearance of the $MbFe^{II}$ oxidation peak, was observed when trichloroacetic acid (TCA) was present

Table 1. Electrochemical Parameters for Myoglobin at 25 °C

pH	sample	reduction peak	$10^7 D'$,[b] $cm^2\ s^{-1}$	$E^{o'}$, V/SCE	$10^3 k^{o'}$, $cm\ s^{-1}$	ref
5.5	Mb-DDAB	Fe^{III}/Fe^{II} [a]	0.5[b]	−0.15	7 ± 1	6
5.5	Mb-DDAB	reduced Fe^{II} [a]	0.3[b]	−1.09	3 ± 1	tw
5−9	aq/bare PG, Pt or Au	Fe^{III}/Fe^{II}			very slow	19a
5−9	aq/bare PG	reduced Fe^{II}	ND	ND	ND	tw
7.0	aq/bare In_2O_3	Fe^{III}/Fe^{II}	0.5	−0.19	0.007	33g
6.5	aq/In_2O_3 hydrophilic	Fe^{III}/Fe^{II} (very pure Mb)[c]	0.5	−0.18	0.3	33a

[a] Solutions contained 50 mM NaBr; tw = this work; ND = not detected. Films on PG electrodes fully loaded with Mb in buffers without dissolved Mb. [b] D_{ct} using measured concentration of Mb and estimated film thickness of 20 μm. [c] Chromatographically purified Mb; all other experiments used ultrafiltration to purify Mb (see Experimental Section).

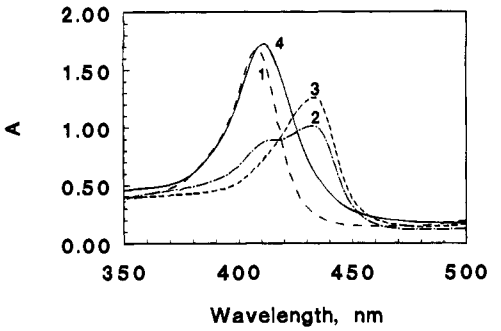

Figure 2. Spectroelectrochemistry of Mb-DDAB films on a tin-doped indium oxide electrode in a pH 5.5 buffer + 50 mM NaBr containing no Mb. Spectra were taken after the following potentials vs SCE were applied for 20 min: (1) 100, (2) −250, (3) −500, and (4) −1250 mV. Film thickness 15−20 μm.

(30) (a) Murray, R. W. In *Electroanalytical Chemistry*; Bard, A. J., Ed.; Marcel Dekker: New York, 1984; Vol. 13, pp 191−368. (b) Bard, A. J.; Faulkner, L. R. *Electrochemical Methods*; Wiley: New York, 1980.

(31) (a) Lexa, D.; Momenteau, M.; Mispelter, J. *Biochem. Biophys. Acta* **1974**, *338*, 151−163. (b) Lexa, D.; Mispelter, J.; Saveant, J.-M. *J. Am. Chem. Soc.* **1981**, *103*, 6806−6812. (c) Kadish, K. M. in *Iron Porphyrins, Part II;* Lever, A. B. P., Gray, H. B., Eds.; Addison-Wesley: Reading, MA, 1983.

(32) Mb-DDAB films on quartz had Soret bands at 413−415 nm. The band found here at 407 nm is influenced by the optical properties of the ITO underlayer.

(33) (a) Taniguchi, I.; Watanabe, K.; Tominaga, M.; Hawkridge, F. M. *J. Elactroanal. Chem.* **1992**, *333*, 331−338. (b) Stargardt, J. F.; Hawkridge, F. M.; Landrum, H. L. *Anal. Chem.* **1978**, *50*, 930. (c) Antonini, E.; Rossi-Bernardi, L.; Chinacone, E., Eds. *Methods in Enzymology;* Academic: New York, 1981; Vol. 76, pp 552−559. (d) Shikama, K.; Matsuoka, A. *J. Mol. Biol.* **1989**, *209*, 489−491. (e) Antonini, E.; Brunori, M. *Hemoglobin and Myoglobin in their Reactions with Ligands;* North Holland: Amsterdam, 1971. (f) King, B. C.; Hawkridge, F. M. *J. Electroanal. Chem.* **1987**, 237, 81−92. (g) King, B. C.; Hawkridge, F. M.; Hoffman, B. M. *J. Am. Chem. Soc.* **1992**, *114*, 10603−10608.

Table 2. Comparison of Positions (λ_{max}, nm) of Mb and Iron Porphyrin Bands in different oxidation states with spectroelectrochemical results[a]

sample (solvent)	Fe(III)	Fe(II)	Fe(I)	ref
C_{12}TPPFeCl (DMF)	422	432	426	31b
$TPPFeClO_4$ (DMSO)	415	430	425	31c
Mb (aq soln)	408−411	434		33a,c,e
ϵ (M^{-1} cm^{-1})	(140 000) (pH 6−9)	(100 000) (pH 7.0)		33f
Mb-DDAB on ITO	408	431 (−500 mV)	411 (−1250 mV)	tw
on quartz	413 (pH 5.5)			6

[a] tw = this work, C_{12}TPPFeCl = a "basket handle" tetraphenylporphyrin iron chloride with two 12 carbon aliphatic chains; $TPPFeClO_4$ = tetraphenylporphyrin iron perchlorate.

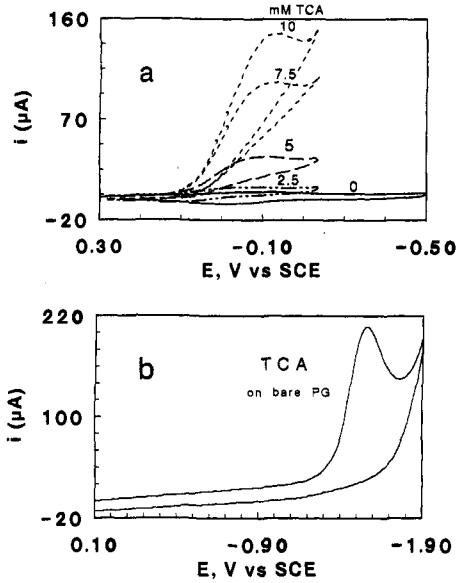

Figure 3. Steady state cyclic voltammograms at 100 mV s^{-1} in pH 5.5 buffer + 50 mM NaBr: (a) Mb-DDAB films with trichloroacetic acid at 0, 2.5, 5, 7.5, and 10 mM; (b) reduction peak for 10 mM TCA on a DDAB-PG electrode (no Mb).

(Figure 3). The $MbFe^{III}$ peak current was linearly proportional to the concentration of organohalide. Results suggest catalytic reduction of TCA via reaction with $MbFe^{II}$. The direct reduction of TCA on a DDAB-PG electrode at about −1.5 V vs SCE at pH 5.5[6] is much more negative than the catalytic peak. Evidence for catalytic reduction at similar potentials was found for ethylene dibromide.

Mb-DDAB films in solutions containing tetrachloroethylene (PCE) or trichloroethylene (TCE) showed little increase in the $MbFe^{III}$ peak (Figure 4). However, a large increase in the more negative reduction peak at −1.1 V was observed, accompanied by the disappearance of the oxidation peak in this potential range. Results are characteristic of catalytic reduction by the more highly reduced Mb. Direct reductions of PCE and TCE on PG occur near −2 V vs SCE.

Mb-DDAB films stored in pH 5.5 buffer containing 10 mM TCA showed decreases in catalytic peak height of about 20% at 100 mV s^{-1} after 1 month. Films of Mb-DDAB were scanned several times daily during this period.

The redox cofactor hemin was also investigated in DDAB films. CV showed that hemin-DDAB films gave a catalytic peak in the presence of organohalides (Figure 5). However, catalytic activity decreased drastically after the first scan. Repetitive CVs in buffer without organohalides present showed

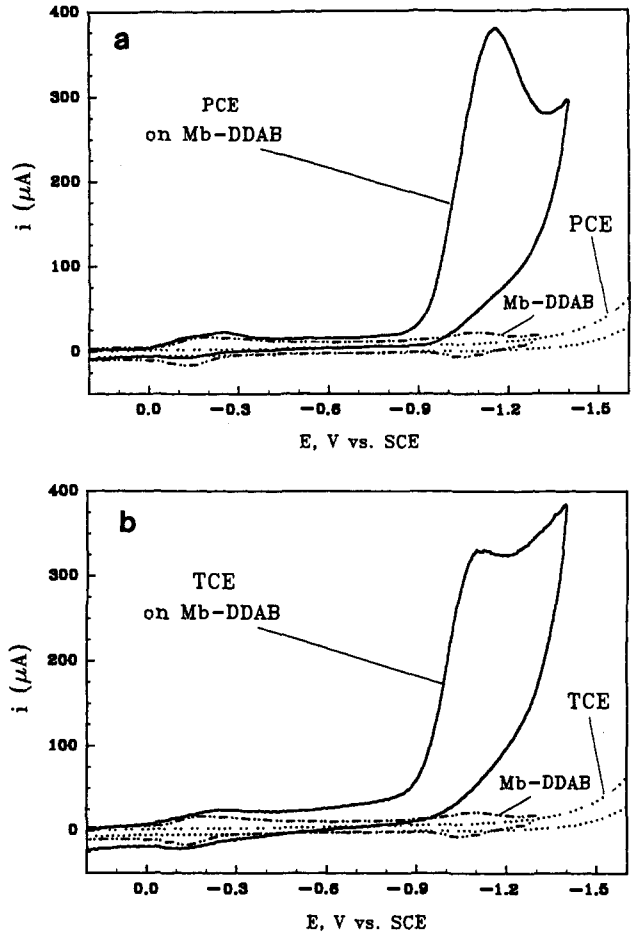

Figure 4. Steady state cyclic voltammograms at 100 mV s^{-1} in pH 5.5 buffer + 50 mM NaBr: (a) Mb-DDAB films on PG with and without 12 mM PCE, and PCE on a DDAB-PG electrode without Mb; (b) Mb-DDAB films on PG with and without 30 mM TCE, and TCE on a DDAB-PG electrode without Mb.

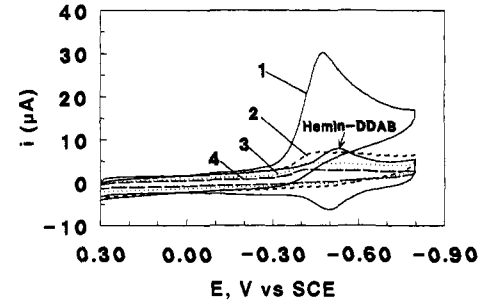

Figure 5. Cyclic voltammograms at 100 mV s^{-1} in pH 5.5 buffer + 50 mM NaBr for hemin-DDAB films with and without 10 mM trichloroacetic acid, showing the instability of reduction current after the first scan. (1) first scan, (2) second scan, (3) third scan, (4) fourth scan. CV without trichloroacetic acid present is labeled hemin-DDAB.

that a major fraction of the hemin leached out of the films after several scans.

Products of Bulk Electrolysis. Solutions containing organohalides were electrolyzed with Mb-DDAB electrodes for 24 h at fixed potentials. In all cases, control experiments without Mb gave no NMR or GC product peaks.

After 5 h bulk electrolysis of trichloroacetic acid (TCA) at −0.4 V vs SCE in deuterated acetate buffer, the NMR of the product mixture (Figure 6) showed peaks corresponding to dichloroacetate, monochloroacetate, and acetate. After 24 h, amounts of monochloroacetate and acetate increased at the expense of dichloroacetate, suggesting stepwise dechlorination of TCA.

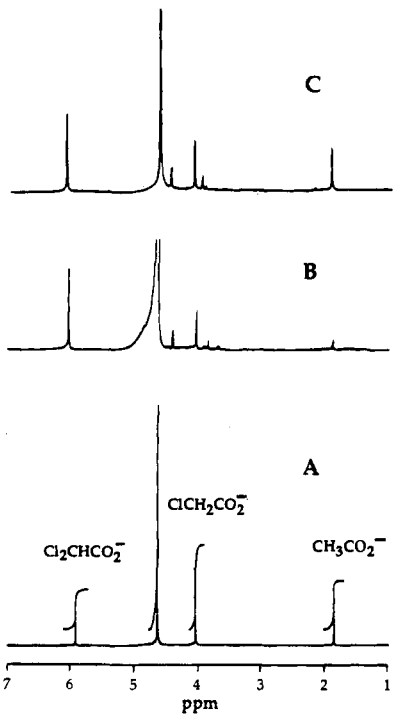

Figure 6. NMR spectra of products from Mb-DDAB-catalyzed reduction of 25 mM TCA in 10 mM deuterated acetate buffer + 50 mM NaBr at pH 5.5 at −0.4 V vs SCE: (a) standards dichloroacetate, monochloroacetate, and acetate, (b) after electrolysis for 5 h, and (c) after electrolysis for 24 h.

NMR confirmed dechlorination of tetrachloroethylene (PCE) and trichloroethylene (TCE), but TCE and (*Z*)-1,2-dichloroethylene have similar chemical shifts. Thus, GC-MS was used for quantitative analyses, and for analysis of reduction products of EDB. Summaries of products found (Table 3) show that one to three halogens were removed from each organohalide. Mb turned over 70−440 times per h during these reductions.

Mb-DDAB films survived electrolyses with a significant fraction of their catalytic activity intact. This was tested by washing electrodes previously used for 24 h and returning them to solutions containing fresh reactant. Current was measured over the first 30 min of a second electrolysis. Results were variable, but used electrodes had currents in second electrolyses of 40−80% of initial values. Some of the variability and loss may be caused by mechanical damage, as evidenced by observance of insoluble film components suspended in solutions after electrolyses.

Kinetics of Organohalide Reductions. The use of computer simulations to obtain rate constants from CV data requires the input of appropriate reaction pathways. Scheme 1 was proposed for catalytic reduction of halogenated acids by the cobalt complex vitamin B_{12}.[16b] It features a two-electron reduction resulting in loss of Cl.

Scheme 1

$$MbFe^{III} + e^- \rightleftharpoons MbFe^{II} \quad k_1^{0\prime}\text{ (at electrode)} \qquad (1)$$

$$MbFe^{II} + Cl_3CCOOH \longrightarrow Cl_2{}^{\bullet}CCOOH + MbFe^{III} + Cl^- \quad (k_1, \text{rds}) \qquad (2)$$

$$MbFe^{II} + Cl_2{}^{\bullet}CCOOH \longrightarrow MbFe^{III} + Cl_2{}^{-}CCOOH \quad \text{(fast)} \qquad (3)$$

$$Cl_2{}^{-}CCOOH + H^+ \longrightarrow Cl_2CHCOOH \qquad (4)$$

Scheme 2

$$MbFe^{III} + e^- \rightleftharpoons MbFe^{II} \quad k_1^{0\prime}\text{ (at electrode)} \qquad (5)$$

$$MbFe^{II} + BrCH_2CH_2Br \longrightarrow BrCH_2CH_2{}^{\bullet} + MbFe^{III} + Br^- \quad (k_1, \text{rds}) \qquad (6)$$

$$MbFe^{II} + BrCH_2CH_2{}^{\bullet} \longrightarrow MbFe^{III} + Br^- + CH_2{=}CH_2 \quad \text{(fast)} \qquad (7)$$

Scheme 3

$$MbFe^{II} + e^- \rightleftharpoons MbFe^{I} \quad k_2^{0\prime}\text{ (at electrode)} \qquad (8)$$

$$MbFe^{I} + Cl_2C{=}CCl_2 \longrightarrow {}^{\bullet}ClC{=}CCl_2 + MbFe^{II} + Cl^- \quad (k_1, \text{rds}) \qquad (9)$$

$$MbFe^{I} + {}^{\bullet}ClC{=}CCl_2 + H_2O \longrightarrow MbFe^{II} + ClHC{=}CCl_2 + OH^- \quad \text{(fast)} \qquad (10)$$

Scheme 2 for reduction of EDB is similar to that proposed for catalytic reduction of alkyl vicinal dibromides by transition metal complexes.[15d−f,16a,c,d] An alternative involves eq 5 followed by a concerted E2 elimination to give olefin directly.[15d,f] Both possible rate determining steps feature the bimolecular reaction of $MbFe^{II}$ with EDB and are kinetically indistinguishable.

Scheme 3 is consistent with product analyses, which confirmed sequential reductive dechlorination for PCE, yielding TCE and (*Z*)-1,2-dichloroethylene. It is similar to other dechlorination pathways proposed for PCE and TCE.[17b,25] The reductant is written as $MbFe^{I}$, but its identity is not yet certain.

For digital simulations of CVs, Schemes 1−3 were represented by a kinetically equivalent simplification. This involved an electron transfer step followed by a bimolecular catalytic rate determining step (rds) (EC′ mechanism) representing reaction between reduced Mb and the organohalide. A second, fast solution electron transfer (SET) representing eq 3, 7, or 9 completes the two-electron dehalogenation. SET is usually energetically favored compared to reduction at the electrode. Thus, all CVs were simulated by using the EC′ (catalytic) pathway with the SET approximation (see Experimental Section).[29] Since the films were much thicker than the diffusion layers generated during CV,[6,19b] diffusion was considered in these simulations.

Table 3. Products of Catalytic Reduction of Organohalides with Mb-DDAB Films[a]

substrate	E_{app}, V vs SCE	turnover no., h^{-1} mol Mb^{-1}	% conversion of reactant	products found	amount found, mmol
Cl_3CCOOH (NMR)	−0.4	440	12	$Cl_2CHCO_2^-$	0.021
				$CClH_2CO_2^-$	0.013
				$CH_3CO_2^-$	0.011
control[b]	−0.4			ND[c]	ND[c]
$BrCH_2CH_2Br$ (GC-MS)	−0.5	120	9	$CH_2{=}CH_2$	0.021
$Cl_2C{=}CCl_2$ (GC-MS)	−1.3	100	25	$ClHC{=}CCl_2$	0.016
				ClHC=CHCl	0.0007
control[b]	−1.3			ND[c]	ND[c]
$ClHC{=}CCl_2$ (GC-MS)	−1.3	70	26	ClHC=CHCl	0.013
control[b]	−1.3			ND[c]	ND[c]

[a] Bulk electrolysis for 24 h using 0.375 mmol TCA, 0.225 mmol EDB, 0.18 mmol PCE, or 0.45 mmol TCE in 15 mL of pH 5.5 buffer. Amount found for PCE and TCE is the sum from analysis of solution and material collected in the cold trap, not corrected for products not trapped. [b] Without Mb. [c] No product peaks detected.

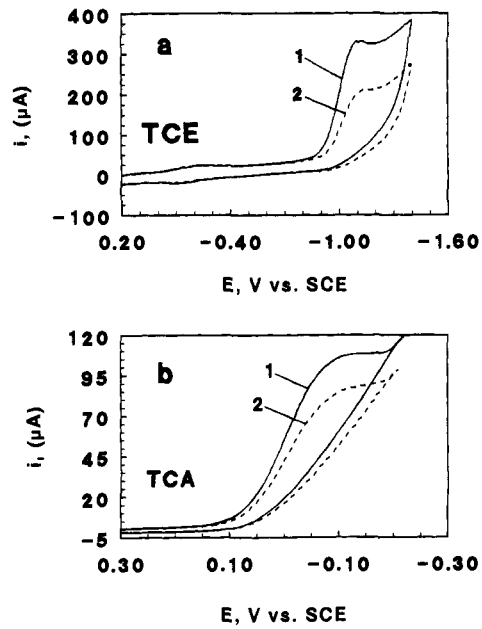

Figure 7. First CV scan after equilibration (1) and steady state scan after repetitive cycling (2) of Mb-DDAB electrodes in pH 5.5 buffer + 50 mM NaBr containing (a) 30 mM trichloroethylene and (b) 10 mM trichloroacetic acid.

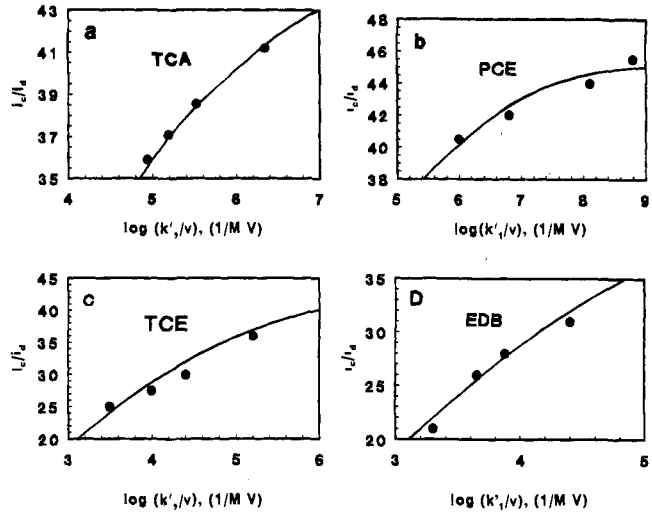

Figure 8. Catalytic efficiencies as i_c/i_d vs log (k_1'/ν) for Mb-DDAB films in 10 mM organohalide solutions plotted (●) for average k_1' values (Table 6) for (a) trichloroacetic acid, (b) tetrachloroethylene, (c) trichloroethylene, and (d) ethylene dibromide. Lines represent theoretical predictions simulated in relevant ranges of k_1'/ν by using the EC′ mechanism with SET approximation (see Experimental Section).

CVs of Mb-DDAB in the presence of organohalides had larger cathodic peak currents on the initial scan than in steady state CVs achieved after many scans (Figure 7). The initial scan reflects the equilibrium concentration of organohalide in the film. After re-equilibration without scanning, the initial scan was reproduced. The smaller steady state peak current reflects the amount of organohalide transported into the films to replace that reacted. Steady state CVs were used for rate estimates.

The current for cathodic $MbFe^{III}$ and $MbFe^{II}$ peaks in solutions containing organohalides is called the catalytic current (i_c). The peak current for Mb-DDAB in the absence of organohalide is i_d. Apparent rate constants were found by comparing experimental i_c/i_d values at a series of scan rates (ν) with appropriate theoretical simulated curves of (i_c/i_d) vs log (k_1'/ν). Good agreement between experiment and simulation was found for all reactants (Figure 8), supporting the EC′ model

Table 4. Voltammetric Data and Apparent Rate Constants for Catalytic Reduction of Trichloroacetic Acid by Mb-DDAB, Acetate Buffer pH 5.5[a]

concn, mM	scan rate, mV/s	E_p, mV vs SCE	i_c/i_d	$10^{-3}k_1'$, M^{-1} s^{-1}
10.0	5	−152	42 ± 3	7.1 ± 1.9
	25	−168	39 ± 2	8.4 ± 0.7
	50	−173	37 ± 2	7.9 ± 1.1
	100	−185	36 ± 2	8.9 ± 0.7
				av 8.1 ± 1.1
7.5	5	−150	29 ± 3	2.1 ± 0.1
	25	−162	26 ± 3	1.9 ± 0.1
	50	−170	25 ± 2	2.5 ± 0.2
	100	−175	24 ± 2	2.3 ± 0.2
				av 2.2 ± 0.1
5.0	5	−145	18 ± 2	0.11 ± 0.01
	25	−155	16 ± 2	0.10 ± 0.01
	50	−156	15 ± 1	0.14 ± 0.02
	100	−165	12 ± 1	0.13 ± 0.02
				av 0.12 ± 0.02
2.5	5	−120	10 ± 1	0.07 ± 0.005
	25	−125	9 ± 1	0.09 ± 0.004
	50	−132	7 ± 1	0.10 ± 0.005
	100	−140	6 ± 1	0.08 ± 0.006
				av 0.085 ± 0.005

[a] Each rate constant is the average for three films given with standard deviations.

Table 5. Voltammetric Data and Apparent Rate Constants for Catalytic Reduction of Organohalides (10 mM) by Mb-DDAB, Acetate Buffer pH 5.5[a]

substrate	scan rate, mV/s	E_p, mV vs SCE	i_c/i_d	$10^{-3}k_1'$, M^{-1} s^{-1}
$BrCH_2CH_2Br$	10	−273	31	0.21
(EDB)	25	−279	28	0.19
	50	−288	26	0.26
	100	−298	21	0.20
				av 0.22 ± 0.03
$Cl_2C{=}CCl_2$	10	−1055	46	14.8
(PCE)	25	−1090	44	14.1
	50	−1120	42	12.8
	100	−1150	40.5	12.0
				av 13.4 ± 1.3
$ClHC{=}CCl_2$	10	−1040	36	11.2
(TCE)	25	−1055	30	10.4
	50	−1070	28	10.0
	100	−1090	25	9.5
				av 10.3 ± 0.7

[a] Each rate constant is the average for two films.

used. Values of k_1' for the various organohalides were independent of scan rate (Tables 5 and 6), also indicating that the model fits the data well. Peak potentials shifted negative with increasing scan rate, also predicted by the EC′ simulations.

The method of obtaining the apparent rate constants k_1' assumes a partition coefficient of unity for the organohalides into the films, which is not accurate. Since a larger solution concentration will drive proportionally more organohalide into the films, k_1' should depend on concentration of organohalide in solution. As expected, an increased concentration of TCA increased the observed k_1' for reaction of TCA with Mb (Table 5).

Rate constants were obtained by spectrophotometry for the reaction of $MbFe^{II}$ in solution with excess EDB and TCA (Table 6). Both reactions fit a pseudo-first-order exponential decay model with less than 75% of the $MbFe^{II}$ reacted.

Discussion

Results demonstrate the use of a protein in a biomembrane-like environment on an electrode to catalyze chemical reactions.

Table 6. Comparison of Reduction Rates of Organohalides

Mb-DDAB films[a]				metal complexes or Mb in soln		
reactant	E^{o}, mV vs SCE	$\Delta E_{1/2}$,[a] mV	k_1', M^{-1} s^{-1}	reductant	E^{o}, mV vs SCE	k_1, M^{-1} s^{-1}
Cl_3CCOOH	−150	1300	8.1×10^3	vitamin B_{12} Co(I)	−760[b,c]	1.5×10^5
				heminFe^{II}−DDAB film^{tw}	−500[a]	80
				MbFe^{II} ^{d,tw}	−150[d]	0.2
$BrCH_2CH_2Br$	−150	1000	2.2×10^2	vitamin B_{12} Co(I)	−760[b,c]	2.6×10^6 [e]
				OEPFe(I)	−1203[e]	1.1×10^5
				[e-(diC_4Ph)-CT-TPPFe(I)]	−1070[e]	4.6×10^5
				OEPCo(I)	−970[e]	6×10^4
				heminFe^{II}Cl	−440 (pH 9)[f]	0.012[g]
				MbFe^{II} ^{d,tw}	−150[d]	0.07
$Cl_2C{=}CCl_2$	−1090	1000	1.3×10^4	vitamin B_{12} Co(I)	−760[b,c]	3.3×10^4 [h]
$Cl_2C{=}CHCl$	−1090	850	1.0×10^4	vitamin B_{12} Co(I)	−760[b,c]	1.3×10^3 [h]

[a] This work (tw), in pH 5.5 buffer containing 50 mM NaBr and 10 mM organohalide; $\Delta E_{1/2}$ represents the difference between potentials of catalytic and direct reduction. Most data are from steady state CVs, except the hemin catalytic rate constant in DDAB film which is from the initial scan. [b] pH 2.3, MeCN−water, ref 16b. [c] pH 2.3, MeCN−water, ref 16c. [d] Solution reactions in pH 5.5 buffer, k_1 obtained by spectrophotometry (ref 4a), $E^{o\prime}$ from ref 33g. [e] In DMF at 20 °C, ref 15f, complexes OEP = octaethylporphyrin; [e-(diC_4Ph)-CT-TPP] = a basket handle tetraphenylporphyrin.[15f] [f] At pH 9 in water hemin is a dimer, from ref 36. [g] Reference 15g. [h] Reference 17b.

By injecting electrons into the film from the electrode, myoglobin was made to act as a redox enzyme. This system provides an easily prepared experimental model for membrane-bound enzyme reactions. These types of experiments could probably be extended to a variety of surfactants and proteins, some of which have already been used to make protein−surfactant films.[5,6,19−22,34]

MbFe^{II} produced in the Mb-DDAB film reduced trichloroacetic to acetic acid and EDB to ethylene (Table 3). These reductions occur at applied potentials 1.0 to 1.3 V less negative than the direct reductions of the organohalides at PG electrodes.

A highly reduced Mb, possibly MbFe^{I} suggested on the basis of spectroelectrochemical results (Figure 2), is responsible for a second reduction peak in Mb-DDAB films. Reduced MbFe^{II} has not been reported previously, to our knowledge. This reduced Mb species converted TCE and PCE to less chlorinated ethylenes (Table 3), with positive shifts in electrode potential of 0.85−1.0 V compared to direct reductions at bare electrodes.

Where comparisons are possible, the products of catalytic electrolyses with Mb-DDAB (Table 3) are the same as those obtained from reductions with cytochrome P450,[14,15g] transition metal complexes,[15−18] and anaerobic bacteria.[25,37] Vinyl chloride, found in microbiological reduction of PCE and TCE,[25] was not found in our systems. If it can be formed by reduction of dichloroethylene using Mb-DDAB films, it must be produced very slowly or lost during product workup.

Apparent rate constants for reductions in 10 mM organohalide solutions were in the range 2×10^2 to 10^4 M^{-1} s^{-1}. These conditional constants are undoubtedly influenced by preconcentration of organohalides into the films. This is reflected in the TCA data, which show that k_1' clearly depends on concentration of reactant (Table 4). In simple DDAB films,[38] preconcentration of 35-fold for dibromocyclohexane and 4-fold for TCA was found. In the present work, initial catalytic peak currents larger than the steady state CV values (Figure 7) suggest that the initial equilibrium concentration of organohalide in the film is decreased by catalytic reduction during multiple scans. In view of the preconcentration, k_1' values can be considered conditional constants proportional to reaction rates.

Rates of reduction of TCA and EDB with MbFe^{II} in the films are smaller than with Co^{I} and Fe^{I} macrocycles in solution (Table 6). However, the organohalide reductions by MbFe^{II} occur at potentials 600 to 1050 mV more positive than with the Co^{I} and Fe^{I} porphyrins and corrins. The reductions catalyzed by MbFe^{II} in the films occur at potentials roughly 1 V more positive than the direct, uncatalyzed reductions, representing a large catalytic decrease in activation energy.

Reduction of EDB and TCA by MbFe^{II} in the surfactant films occurs at rates thousands of times faster than by MbFe^{II} in solution (Table 6). Reduction of TCA with the unstable hemin-DDAB films gave an initial rate constant 100 times smaller than the k_1' for MbFe^{II}-DDAB, but 400 times faster than reaction of TCA with MbFe^{II} in solution. Catalysis in hemin-DDAB films is also probably facilitated by reactant preconcentration.

Reduction rates of PCE and TCE with the highly reduced Mb species at −1.1 V are comparable to those of the Co^{I} corrin complex vitamin B_{12s} (Table 6). We cannot compare these rates with reactions in solution, because the more highly reduced Mb was not accessible in solution.

Enhancement of reaction rates for EDB and TCA in the Mb-DDAB films can be attributed partly to preconcentration of the organohalide reactant, which increases the observed rate because the rate determining step is second order.[39] However, interactions between surfactant and protein may also play a role in controlling reactivity. Kunitake and co-workers found a greatly enhanced rate of autooxidation for MbFe^{II}-O_2 bound to surfactant bilayer vesicles.[5] The same group found that *N*-demethylase activity is enhanced 10-fold when cytochrome *c* is bound to vesicles of phosphate surfactants but is not influenced by vesicles of ammonium surfactants.[40] Also, rates of catalysis by membrane-bound cytochrome P450 depend on the lipid composition of the membrane.[10,41] Thus, the protein−surfactant films discussed herein may have several possible mechanisms for reactivity control, including preconcentration of reactants based on hydrophobic and Coulombic interactions with the film[42] and variation of surfactant type to control surfactant−protein interactions.

(34) Huang, Q.; Lu, X.; Rusling, J. F. Ms. In preparation.
(35) Rusling, J. F.; Zhang, H.; Willis, W. S. *Anal. Chim. Acta* **1990**, *235*, 307−315.
(36) Bednarski, T. M.; Jordan, J. *J. Am. Chem. Soc.* **1967**, *89*, 1552−1557.
(37) (a) Abelson, P. H. *Science* **1990**, *250*, 733. (b) Arciero, D.; Vannelli, T.; Logan, M.; Hooper, A. B. *Biochem. Biophys. Res. Commun.* **1989**, *159*, 640−643. (c) Fathepure, B. Z.; Nengu, J. P.; Boyd, S. A. *Appl. Environ. Microbiol.* **1987**, *53*, 2671−2674. (d) Bouwer, E. J.; McCarty, P. L. *Appl. Environ. Microbiol.* **1983**, *45*, 1286−1294.
(38) Preconcentration cannot be measured directly by CV in the Mb-DDAB films, because catalytic reactions interfere with the direct reductions.
(39) Rusling, J. F. *Acc. Chem. Res.* **1991**, *24*, 75−81.
(40) Hamachi, I.; Fujita, A.; Kunitake, T. *J. Am. Chem. Soc.* **1994**, *116*, 8811−8812.
(41) Ingleman-Sundberg, M. In *Cytochrome P450*; Ortiz de Montellano, P. R., Ed.; Plenum: New York, 1986; pp 119−160.
(42) Rusling, J. F. *Microporous Mater.* **1994**, *3*, 1−16.

Conclusions

Stable Mb-DDAB films on electrodes can catalyze reductions of organohalide pollutants with significant lowering of activation free energy. Rates for organohalide reductions in these films are thousands of times larger than in solution and are enhanced partly by preconcentration of organohalides in the films. The films provide a biomembrane-like environment for these biologically relevant reactions. Furthermore, a reduced form of $MbFe^{II}$ can be produced in the films.

Mb−surfactant films appear to provide good models for reactions of the membrane-bound enzyme cytochrome P450, which dehalogenates organohalides by reductions and oxidations in living systems.[7] Also, the films may be applicable as the basis for chemical sensors and synthetic catalysts.

Acknowledgment. This work was supported by U.S. PHS Grant No. ES03154 from NIH awarded by the National Institute of Environmental Health Sciences. The authors are grateful to Professor T. Kunitake of Kyushu University, Japan, for helpful discussions and to the Environmental Research Institute at the University of Connecticut for GC-MS analyses.

JA952074U